



Published in final edited form as:

Langmuir. 2012 January 10; 28(1): 548–556. doi:10.1021/la202053k.

A surface derivatization strategy for combinatorial analysis of cell response to mixtures of protein domains

Chunyi Chiang¹, Stella W. Karuri³, Pradnya P. Kshatriya², Jeffrey Schwartz⁴, Jean E. Schwarzbauer⁵, and Nancy W. Karuri^{2,*}

¹Illinois Institute of Technology, Department of Biological, Chemical and Physical Sciences, Chicago, IL, 60616

²Illinois Institute of Technology, Department of Chemical and Biological Engineering, Chicago, IL, 60616

³National Cancer Institutes, Biometrics Research Branch, Rockville, MD 20852

⁴Princeton University, Department of Chemistry, Princeton, NJ 08544

⁵Princeton University, Department of Molecular Biology, Princeton, NJ 08544

Abstract

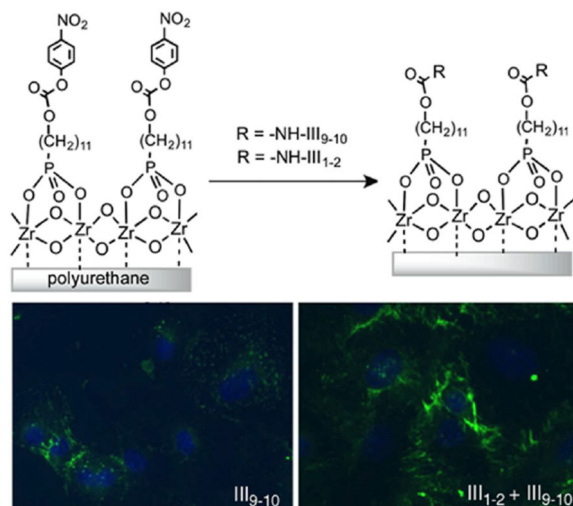
We report a robust strategy for conjugating mixtures of two or more protein domains to non-fouling polyurethane surfaces. In our strategy, the carbamate groups of polyurethane are reacted with zirconium alkoxide from the vapor phase to give a surface bound oxide that serves as a chemical layer that can be used to bond organics to the polymer substrate. An hydroxyalkylphosphonate monolayer was synthesized on this layer, which was then used to covalently bind primary amine groups in protein domains using chloroformate-derived cross-linking. The effectiveness of this synthesis strategy was gauged by using an ELISA to measure competitive, covalent bonding of cell-binding (III₉₋₁₀) and fibronectin-binding (III₁₋₂) domains of the cell adhesion protein fibronectin. Cell adhesion, spreading, and fibronectin matrix assembly were examined on surfaces conjugated with single domains, a 1:1 surface mixture of III₁₋₂ and III₉₋₁₀, and a recombinant protein “duplex” containing both domains in one fusion protein. The mixture performed as well or better than the other surfaces in these assays. Our surface activation strategy is amenable to a wide range of polymer substrates and free amino group-containing protein fragments. As such, this technique may be used to create biologically specific materials through the immobilization of specific protein groups or mixtures thereof on a substrate surface.

Graphical abstract

*Corresponding author. 10 West 33rd Street, Chicago, IL 60610, Tel.: 1 312 567 3262; fax: 1 312 567 3874, nkaruri1@iit.edu.

SUPPORTING INFORMATION AVAILABLE

Supporting information includes protein characterization studies (Supplementary Figure 1) and a comparison study of surfaces conjugated with FN and III₉₋₁₀ (Supplementary Figure 2). This information is available free of charge via the Internet at <http://pubs.acs.org/>.



Keywords

fibronectin; surface chemistry; zirconium oxide; cell adhesion; extracellular matrix; integrin; polyurethane

INTRODUCTION

Considerable research has focused on modifying the physical and chemical properties of synthetic materials in an attempt to mimic the properties of tissue extracellular matrices (ECMs). Most of these modifications have been designed to facilitate cell adhesion and to provide physical and biochemical stimuli that are important for cell growth and tissue development. A fibronectin (FN)-rich ECM plays a critical role in the development and repair of most tissues¹, and it is an ideal model system for the design of synthetic scaffolds that support cell adhesion and growth.

FN is a large, ubiquitous ECM protein that is formed into extensive fibrillar networks within tissues and presents binding sites for other ECM molecules including itself, and for cell surface receptors such as integrins. These binding domains are composed of structurally homologous modules that are classified as type I, II or III (see Figure 1A)². Scaffold design strategies using FN biochemistry have focused on the immobilization of peptides derived from the FN cell-binding domain III₉₋₁₀, specifically the Arginine-Glycine-Aspartic acid (RGD) sequence in III₁₀ and its Proline-Histidine-Serine-Arginine-Asparagine synergy site in III₉³⁻⁵. Other studies have focused on immobilizing fragments spanning III₉₋₁₀⁶⁻¹⁰. The impetus for immobilizing the functional domain as opposed to RGD or full-length FN is that it results in higher biological activity and receptor selectivity⁶⁻⁸. However, FN not only binds to cells but also has domains that bind other FN molecules and that can activate ECM assembly. The presence of these multiple stimuli work collectively to influence cellular responses. Of particular interest is the III₁₋₂ domain which binds other FN molecules and is important for the establishment of a fibrillar ECM¹¹. Whereas, there are different functional domains in FN that collectively contribute to its biological activity, the potential to create

synthetic materials with cell binding and FN binding stimuli derived from FN has yet to be fully explored.

Mixtures of polypeptides derived from or spanning III₁₋₂ and III₉₋₁₀ have been coated on surfaces as single or coupled units^{9, 10}. Surfaces coated with a fragment of III₁ coupled to III₈₋₁₀ have been shown to have higher adhesion and spreading compared to those coated with FN⁹ in FN-null mouse embryonic fibroblasts. These cells cannot produce FN but can assemble it into an ECM if it is provided in culture media. Others have shown that the assembly of FN into an ECM in FN-null fibroblasts on FN surfaces coated with III₁, a fragment III₇₋₁₀ and the C-terminal FN fragments is comparable to those coated with full length FN¹⁰. Two questions stand out from these studies that need to be addressed. These are: (i) what are the individual and collective roles of III₁₋₂ and III₉₋₁₀ on cell adhesion and ECM assembly and (ii) what are the differences in cellular responses to surfaces where the two domains are immobilized as a mixture and those where they are coupled to the surface as a single polypeptide.

Key design variables for generating biofunctional materials from synthetic scaffolds include the robustness of the surface immobilization method, and the temporal stability of the material. In terms of stability, polypeptides covalently linked to synthetic materials are more stable and biologically active than those coated on surfaces. Adsorbed polypeptides can be denatured, desorbed from the surface or exchanged from the surface by protein constituents in the culture media or those secreted by cells¹². It was therefore interesting to compare how plated cells respond to biologically inert materials conjugated with FN domains that interact with cell receptors and those that bind other FN molecules.

We now report a robust and versatile surface chemistry approach for simultaneous derivatization of polymer scaffolds both with a FN-binding and a cell-binding domain (III₁₋₂ and III₉₋₁₀, respectively). This approach uses zirconium tetra(*tert*-butoxide) as the precursor of a zirconium oxide chemical layer that bonds to the surface of non-fouling polyurethane and that has been shown to enable high peptide loadings on this polymer¹³; it demonstrates a straightforward approach to conjugate these larger polypeptides of FN through lysine amino acid residues. We also show that surfaces conjugated with both III₁₋₂ and III₉₋₁₀ have higher cell adhesion and ECM assembly than surfaces with the individual domains. We have engineered a recombinant protein with both III₁₋₂ and III₉₋₁₀ and show that an equimolar mixture of III₁₋₂ and III₉₋₁₀ immobilized on the surfaces yields a comparable biological response as the recombinant polypeptide that contains one of each domain. This strongly suggests that a combinatorial approach can be employed to direct multiple biological responses by varying the amounts of the FN and cell-binding domains. Since our surface chemistry approach is easily applicable to a wide variety of polymers and to different combinations of protein domains, our results suggest that a combinatorial approach, in which a variety of protein domains are simultaneously bonded to a substrate in various ratios, might be used to control biological responses on a surface and thus provide the means to manipulate these responses.

MATERIALS AND METHODS

Production and Purification of individual III₁₋₂, III₉₋₁₀ and III₁₋₂III₉₋₁₀

We have in our laboratory constructs of III₁₋₂ and III₉₋₁₀ expressed as glutathione S-transferase (GST) fusion proteins in *Escherichia coli* DH12α. A construct of III₁₋₂III₉₋₁₀ was generated as follows. PCR amplification products encoding III₁₋₂ and III₉₋₁₀ were generated using human FN cDNA as template. Products were inserted into the pGEX-6P-2 vector (GE Lifesciences, Piscataway, NJ) for expression of GST-III₁₋₂ and GST-III₉₋₁₀ fusion proteins. A single fusion protein containing both domains (III₁₋₂III₉₋₁₀) was created using overlap extension PCR. This consists of a first PCR with primers flanking the termini of the III₁₋₂ domain in pGEX-6P-2, but excluding the stop codon at the 3'-end, and primers flanking III₉₋₁₀ in pGEX-6P-2. The primers at the 5' end of III₁₋₂ and those at the 3' end of III₉₋₁₀ were designed with BglII and SalI restriction sites respectively. The second PCR used the two PCR products from the first and second reactions and the aforementioned 5'-primer of III₁₋₂ template and the 3'-primer of III₉₋₁₀ template. The final PCR products were cloned into the pGEM vector (Promega, Madison, WI) to generate pGEM-III₁₋₂III₉₋₁₀, which was subsequently cloned into the BamHI and Sal sites of pGEX-6P-2.

All of the constructs were expressed as GST fusion proteins in *E. coli* DH12α (Figure 1B). The proteins were purified by affinity chromatography on glutathione-Sepharose 4 Fast Flow (GE Lifesciences) following the manufacturer's specifications and then dialyzed into phosphate buffered solution (PBS, Fisher Scientific, Pittsburg, PA). After purification, the proteins were characterized through sodium dodecyl sulfate polyacrylamide gel electrophoresis or SDS-PAGE (Supplementary Figure 1A) and immunoblotting (Supplementary Figure 1B). The SDS-PAGE and immunoblotting studies showed the expected molecular components and confirmed the molecular weights of III₁₋₂, III₉₋₁₀ and III₁₋₂III₉₋₁₀. Prior to their addition to the activated surfaces the proteins were diluted to the appropriate concentration using sodium phosphate-saline solution (137 mM NaCl, 2.7 mM KCl, 10 mM Na₂HPO₄, 1.76 mM KH₂PO₄, pH 9).

Polyurethane casting and surface chemistry

Thin films of polyurethane on glass cover slips were created by dissolving 0.3 grams of polyurethane (Sigma-Aldrich, St. Louis, MO) in 10 ml of 88% formic acid (Fisher) and spin coating the polymer solution on 12 mm glass cover slips (Fisher) at 3500 revolutions/minute. We found that deposition of a layer of zirconium tetra(*tert*-butoxide) (**1**) (Sigma-Aldrich) on the glass cover slips followed by heating helped to improve the adhesion between polyurethane and glass¹⁴. The polyurethane coated glass coverslips were air dried for five minutes at room temperature and then a further five minutes at 120 °C. The samples were then cooled and placed in a vacuum chamber with a vacuum and vapor inlet. The chamber was evacuated, the vacuum valve closed and the polyurethane coated glass coverslips were exposed to two cycles of zirconium tetra(*tert*-butoxide) (**1**) deposition for five minutes at a time (Figure 1C) by repeatedly opening and closing the vapor and vacuum inlet valves. After the last deposition step, the samples were heated to 45 °C and held at this temperature for five minutes to convert the zirconium alkoxide layer to a cross-linked mixed alkoxide-oxide. Samples were then cooled and further converted to the cross-linked oxide

chemical adhesion layer (**2**) by heating in a microwave oven for 30 seconds under high power (Figure 1C)¹⁵. The samples were then suspended vertically in a 0.1 mM solution of 11-phosphoundecanol (**3**) in ethanol (Figure 1C), and the solution was allowed to evaporate. This formed an organized phosphonic acid monolayer^{16, 17}, which was stabilized on the Zr oxide surface as a phosphonate (**4**) by heating in a microwave oven at high power for five minutes. The samples were then washed in ethanol to remove unbound **3**, air-dried, and placed in a round bottom flask under flowing argon for 10 minutes to ensure a moisture free environment. Then p-nitrophenyl chloroformate was coupled to **4** in dry diethyl ether (Sigma-Aldrich) in the presence of diethylamine (Sigma-Aldrich) under argon gas for 1 hour. Dry conditions are necessary to obviate hydrolytic side reactions.

Following a reaction with the chloroformate which gives **5** the samples were quickly rinsed in ethanol and immersed in peptide or protein solutions in a sodium phosphate solution at pH 9 (Figure 1C). Protein solutions for assays of III₁₋₂ and III₉₋₁₀ were in the range of 0–5 μ M of the GST fusion proteins. Human plasma FN was used as a control at concentrations of 0–0.5 μ M. After an incubation of one hour at room temperature in the protein solutions, the samples (Figure 1C, **8**) were passivated by immersing in a solution of 100 mM Tris-HCl at pH 8.8 to hydrolyze unreacted carbonate groups. Prior to cell culture the samples were rinsed with PBS, blocked with 1% bovine serum albumin (Sigma-Aldrich) in PBS for an hour at room temperature and then washed three times with PBS. Blocking prevents non-specific adsorption of serum components.

Coating surfaces with GST-III₉₋₁₀

Surfaces were coated with III₉₋₁₀ to compare the response of cells to functionalized surfaces to that of surfaces where the proteins were non-specifically adsorbed. The surfaces used for protein coating were unfunctionalized polyurethane surfaces. The concentration of III₉₋₁₀ used was 0.5 μ M and the protein was in sodium phosphate-saline solution. The coating time was done for one hour at room temperature. Following coating the surfaces were treated in a similar manner as functionalized surfaces **8** in Figure 1C.

Surface characterization

During the chemical coupling steps shown in Figure 1C the surface was characterized by surface wettability through contact angle measurements. The quantity of protein on the surface was measured via ELISA assays using monoclonal antibody HFN7.1, which recognizes human FN near the cell-binding site. For ELISAs, the control surface consisted of the carbonate terminated surface **6** in Figure 1C.

Cell adhesion and spreading assays

Cell adhesion and spreading were evaluated *in vitro*. NIH3T3 mouse fibroblasts maintained in Dulbecco's Modified Eagle's Medium (Invitrogen, Carlsbad, CA) with 10% bovine calf serum (Fisher) were prepared for cell adhesion experiments as previously described. Cells were trypsinized and a 0.5 ml suspension at a density of 2×10^4 cells/ml in serum-free DMEM was added to the each sample in a 24 well plate. After 60 minutes, the media with non-adherent cells was removed, the cells were washed twice with PBS, fixed in 3.7 % paraformaldehyde (Fisher) in PBS and permeabilized with 0.5% NP-40 (Fisher) in PBS.

After rinsing with PBS, actin and cell nuclei were stained with fluorescein-conjugated phalloidin (Invitrogen) at a dilution of 1:50 and 1 $\mu\text{g/ml}$ Hoechst (Invitrogen) in 2% ovalbumin (Sigma-Aldrich) in PBS. The samples were washed three times in PBS, followed by a last wash in water and mounted using prolong antifade (Invitrogen) and imaged. Imaging was done with a Carl Zeiss LSM 510 microscope (Carl Zeiss, Thornwood, NY).

Image analysis

Cell adhesion and spreading were quantified with Image J software. For cell adhesion, images were generated by the image capture software, Axiovision, a Hoechst filter and a 10 \times objective. Image J was used to extract cell number from the distribution of the monochrome images of the nuclei. At least four areas per sample were examined. For cell area the raw images generated by Axiovision were opened with Image J software and thresholded to produce monochrome signals. Cell area was extracted as the area of the pixilated areas. The cell area images were compared to images collected with the Hoechst filter to determine a pixilated area per cell, which was then converted to μm^2 area per cell.

Immunofluorescence of extracellular FN

NIH3T3 mouse fibroblasts in DMEM supplemented with 10% bovine calf serum (BCS, Hyclone) were grown to 90% confluency, trypsinized and resuspended in DMEM media. Cells numbering 2×10^5 were added per sample in a 24 well dish and incubated for half an hour. After 30 minutes the media and non-adherent cells were removed and fresh media supplemented with 10% BCS was added. The samples were then incubated for 3, 6, 12 and 24 hours. After incubation, the samples were rinsed twice with PBS, fixed in 3.7% paraformaldehyde and labeled for extracellular FN with polyclonal antibodies R457 against the 70 kDa amino-terminal domain of FN at a dilution of 1:100 in 2% ovalbumin in PBS. The antibodies used in these studies detect the 70kDa amino-terminal of FN and would bind full-length FN and not the immobilized FN domains. After a 30 minute incubation period at 37 $^\circ\text{C}$, the samples were washed with PBS and incubated with goat anti rabbit antibodies conjugated to fluorescein (Invitrogen). The samples were then rinsed in several PBS washes followed by water, then mounted and imaged. The samples were imaged with a Carl Zeiss LSM 510 microscope with fluorescein filter under a 20 \times objective. The optimum exposure time was obtained for the strongest signal at an intensity that was not saturated and kept constant during sample imaging. This was to ensure that for the different treatments fluorescence intensity was dependent on FN abundance and not microscopy settings.

Statistical Analysis

Experiments were performed a minimum of three times. The data presented are the means \pm the standard error of the mean of at least two of the experiments. An analysis of variance was conducted to examine whether III₁₋₂ and III₉₋₁₀ surface composition had a significant effect on cell adhesion and spreading. Where different treatments were compared, a Student's t-test was used. P values < 0.05 were considered statistically significant.

RESULTS

Functionalization and characterization of polyurethane surfaces with FN domains

A modular approach was used to functionalize polyurethane surfaces with FN domains. We bound the III₁₋₂ and III₉₋₁₀ FN domains individually (Figure 1Bi and 1Bii) and collectively (Figure 1Biii and 1Biv) on polyurethane surfaces. We focused on two approaches to mix III₁₋₂ and III₉₋₁₀ on a surface. The first was a combinatorial one, where individual III₁₋₂ and III₉₋₁₀ domains were covalently bound to the activated polyurethane surface from a one-to-one mixture in solution (Figure 1Biii). In the second, we fused the cDNAs encoding III₁₋₂ and III₉₋₁₀ to code for a single protein with two domains linked by a short, flexible amino acid spacer (Figure 1Biv). This fusion protein was then conjugated to the activated surface. The FN type III modules that comprise III₁₋₂ and III₉₋₁₀ are homologous in structure and consist of polypeptide chains that fold into ellipsoidal β -barrel structures^{18, 19}, represented by the ovals in Figure 1B. To facilitate the isolation of these proteins from *E. coli* bacterial lysates, the cDNAs for the FN domains were fused to the GST gene, and the FN domains, as GST fusion proteins, were then covalently bound to the polyurethane surface.

In a stepwise approach, the FN domains were covalently bonded to the surface via a carbonate derivative (**6**) of a phosphonate (Figure 1C). Surface wettability was used to characterize the surfaces at each synthesis step. Contact angles for water wetting of polyurethane, zirconium oxide- (**2**), phosphonate- (**4**) and carbonate-terminated (**6**) surfaces were 64°–68°, 48°–54°, 70°–80°, and 80°–90°, respectively. The decrease in contact angle from polyurethane to the surface oxide is due to an increase in the oxygen content of the surface. Hydrophobicity increases with the addition of the pendant alkyl groups after treatment of the surface oxide with PUL and remains high following chloroformate treatment due to the presence of the large hydrophobic phenyl groups.

Enzyme-linked immunosorbent assays (ELISAs) with antibodies that bind the III₉₋₁₀ domain were used to determine the relationship between solution and surface protein concentration. The amount of III₉₋₁₀ coupled to the surface varied with its concentration in solution (Figure 2A). In particular, the amount of III₉₋₁₀ detected on the surface of the activated polyurethane increased with concentration from 0 to 1 μ M; above 1 μ M, the ELISA absorbance did not change with increasing solution concentration. The raw absorbance readings were within the linear range of the spectrophotometer and the 1 μ M solution concentration was taken to correspond to the saturation point of III₉₋₁₀ groups on the activated surface.

III₁₋₂ and III₉₋₁₀ have similar molecular weights and domain structures^{18, 19} so it seems likely that surface coupling of these two proteins is equivalent. We do not have antibodies specific to III₁₋₂ that can be used for an ELISA and could not directly determine its loading on an activated surface. Therefore, we carried out a competition experiment to determine if these two proteins showed the same relative rates of bonding to an activated surface. Domains were bonded from mixture solutions under conditions where total protein was kept constant at 1 μ M and the amount of III₉₋₁₀ on the surface was measured through ELISA (Figure 2B). The data from three separate experiments, each conducted in duplicate, can be fit to a straight line (slope = 0.86, intercept = 0.05, regression value = 0.98). The confidence

interval of the regression of the slope in Figure 2B includes one indicating that the slope is likely equal to one. This means that for an equimolar mixture of III₁₋₂ and III₉₋₁₀, where the total protein concentration is 1 μ M, half of the protein bonded on the surface is III₁₋₂ and the other half is III₉₋₁₀. Collectively, these data strongly suggest that III₁₋₂ and III₉₋₁₀ have similar binding with the activated polymer surface.

Based on ELISA results, four surface conditions were chosen to examine the individual and collective effects of III₁₋₂ and III₉₋₁₀ on cell behavior. Individual domains were investigated by using a 0.5 μ M solution concentration of either III₁₋₂ or III₉₋₁₀. To probe the combined effect of III₁₋₂ and III₉₋₁₀ we used the 1:1 *Mix* condition shown in Figure 1B, which resulted in equimolar amounts of surface attachment of III₁₋₂ and III₉₋₁₀. As a basis for comparison with the fusion protein, we used a 0.5 μ M solution of III₁₋₂III₉₋₁₀ so that the total number of III₁₋₂ and III₉₋₁₀ groups would be comparable to the *Mix* solution. An ELISA to detect bound III₉₋₁₀ showed similar amounts of protein on surfaces coupled with solutions of III₉₋₁₀, *Mix*, and III₁₋₂III₉₋₁₀ proteins (Figure 2C).

Cell attachment and spreading on functionalized polyurethane

Cell adhesion was used as a probe for changes in surface chemistry after each step shown in Figure 1C. NIH3T3 fibroblasts in serum-free media were cultured for 1 hr on surfaces terminated with polyurethane, phosphonate **4**, carbonate **6** and III₉₋₁₀ (**8a**), then fixed and stained with fluorescent phalloidin to visualize the actin cytoskeleton. Robust cell adhesion and spreading were observed when cells were cultured on surfaces terminated with III₉₋₁₀ (Figure 3A). A quantitative analysis of cell spreading demonstrated that polyurethane surfaces and surfaces terminated with PUL or carbonate (**4** and **6**) had significantly less cell adhesion and spreading compared to surfaces functionalized with III₉₋₁₀ (Figure 3Bi and 3Bii, respectively).

We examined the efficacy of our surface modification chemistry by comparing the adhesion response of cells on III₉₋₁₀ functionalized surfaces with that on surfaces with III₉₋₁₀ adsorbed from solution. Both surface treatments used a GST-III₉₋₁₀ solution concentration of 0.5 μ M. From ELISA assays it was determined that there was 40% more III₉₋₁₀ on the functionalized surfaces than on the coated surfaces (data not shown) suggesting that the rate of surface-immobilization of protein is increased by chemical bonding compared to adsorption. Figure 3C shows that cells attached and spread on surfaces with either treatment. The average number of adherent cells was comparable for the two types of surfaces (Figure 3Di). However, the average cell area on surfaces to which III₉₋₁₀ was covalently bound was more than twice that on surfaces with adsorbed III₉₋₁₀ (Figure 3Dii), probably due to the higher level of bonded protein. These results show that covalent bonding of III₉₋₁₀ onto surfaces increases the amount of functional groups on a surface and allows increased cell spreading compared to III₉₋₁₀ adsorption.

We compared surfaces bonded with FN to those bonded with III₉₋₁₀ at different solution concentrations (Supplementary Figure 2). Although FN is approximately ten times larger than III₉₋₁₀ in molecular weight, we found that the surface amount detected by ELISA using monoclonal antibodies was much higher than that of III₉₋₁₀ at comparable solution concentrations (Supplementary Figure 2A). This may be due to changes in FN conformation

when in contact with the hydrophobic surface that lead to FN aggregation. As expected, the larger molecule, FN, saturates the surface at a lower concentration than III₉₋₁₀. At 0.5 μM solution concentration, which corresponds to surface saturation of FN (Supplementary Figure 2A) and approximately 80% surface coverage of III₉₋₁₀ (Figure 2A), cell adhesion was comparable between the two surfaces (Supplementary Figure 2B). Therefore, III₉₋₁₀ functionalized surfaces support cell adhesion in a manner comparable to that of surfaces functionalized with full-length FN.

The influence of III₉₋₁₀ and III₁₋₂ functionalized surfaces (**7a** and **7b** in Figure 1C) on cell adhesion and spreading was examined through cell adhesion assays. Cells attached and spread on surfaces that had III₉₋₁₀ alone or had both domains attached (Figure 4A, *Mix* or III₁₋₂III₉₋₁₀), but did not attach to surfaces covalently treated with III₁₋₂ alone (Figure 4A, III₁₋₂). Interestingly, whereas bound III₁₋₂ alone did not support cell adhesion, its presence on surfaces with III₉₋₁₀ resulted in statistically significantly greater cell adhesion compared to surfaces activated only with III₉₋₁₀ (Figure 4B). Apparently, the presence of III₁₋₂ enhanced the cell-surface interactions whether as a 1:1 mixture or as a fusion protein. Thus, an enhanced effect of mixing the domains is apparent. This effect cannot be attributed to surface concentrations of III₉₋₁₀ as ELISAs showed that, on average, the concentration of III₉₋₁₀ in the two treatments is comparable (Figure 2D). Cell spreading on functionalized surfaces was comparable on polyurethane surfaces terminated with III₉₋₁₀ alone and where III₉₋₁₀ was mixed with or linked to III₁₋₂ (Figure 4C). Cells on III₁₋₂ and the nitrophenyl carbonate terminated polyurethane surfaces (*ctrl* in Figure 4C) exhibited significantly less spreading than cells on surfaces containing III₉₋₁₀.

The potentiation of III₉₋₁₀ activity by III₁₋₂ may involve the effect of III₁₋₂ on substrate surface chemistry and therefore the binding affinity between III₉₋₁₀ and α5β1 integrins. Cells may be more adherent to a III₉₋₁₀ functionalized surface in the presence of a protein background, which is provided by III₁₋₂, than on a nitrophenyl carbonate background. Changes in the surface microenvironment can alter protein conformation and activity¹². To better understand the effect of III₁₋₂ on III₉₋₁₀ activity, we compared a mixture of III₁₋₂ and III₉₋₁₀ with a mixture of III₉₋₁₀ and GST. The surface amount of III₉₋₁₀ in the mixtures and for III₉₋₁₀ alone treatments was determined by ELISA and is shown in Figure 5A. A solution mixture of 0.5 μM GST and 0.5 μM III₉₋₁₀ had more surface bound III₉₋₁₀ than a mixture of 0.5 μM III₁₋₂ and 0.5 μM III₉₋₁₀. When the solution mass concentration of GST in a mixture with III₉₋₁₀ was matched to that of III₁₋₂ by doubling its solution concentration to 1.0 μM, the amount of III₉₋₁₀ on the surface was comparable to that obtained with III₁₋₂ and III₉₋₁₀ mixture condition. A GST and III₉₋₁₀ mixture and a mixture of III₁₋₂ and III₉₋₁₀ presenting a similar amount of cell binding sites had comparable adhesion which was significantly higher than III₉₋₁₀ alone (Figure 5B). In control studies surfaces functionalized with GST alone did not support cell adhesion (data not shown). This indicates that the effect of mixing III₁₋₂ or GST with III₉₋₁₀ on a surface is the modification of surface chemistry to present a more conducive environment for cell attachment. The density of the protein groups on the surface is high and mixing III₉₋₁₀ with GST or III₁₋₂ may have the effect of changing III₉₋₁₀ conformation such that it has a higher binding affinity for cells.

FN matrix assembly on functionalized surfaces

Fibronectin matrix assembly is initiated by integrin binding to the III₉₋₁₀ domain of FN, and the extent of fibril formation is regulated by interactions involving the III₁₋₂ domain^{2, 11}. The effect of surfaces with bound III₁₋₂ and III₉₋₁₀ on the formation of FN fibrils was investigated through fluorescence microscopy. Figure 6 shows a time course immunofluorescence images of extracellular FN in NIH3T3 mouse fibroblasts cultured on substrates variously treated for 3, 6, 12 and 24 hours. The source of extracellular FN assembled in the ECM is that synthesized by cells^{20, 21}. At 3 hr after plating, some punctate staining was observed in cells on surfaces terminated with III₉₋₁₀ alone, whereas short fibrils were already apparent on a mixture of III₁₋₂ and III₉₋₁₀ (Figure 6). By 12 and 24 hour time points, longer fibrillar structures were evident in cells on both surfaces. The intensity of the stain was higher on surfaces terminated with a mixture of both domains than on surfaces derivatized with III₉₋₁₀ alone. The difference in fibril numbers on III₉₋₁₀ and the mixture at early times suggests that presenting two domains on the surface may increase the rate of initiation of fibril assembly or of fibril growth once assembly has begun. In control studies, the amount of extracellular matrix FN was higher in cells cultured on surfaces with a mixture of III₁₋₂ and III₉₋₁₀ than on surfaces with GST and III₉₋₁₀ and this difference decreased with time (data not shown). Therefore, mixing III₁₋₂ and III₉₋₁₀ results in higher FN matrix assembly than with III₉₋₁₀ alone and this effect is specific for III₁₋₂.

DISCUSSION

The main objective of this study was to covalently bond FN domains onto a non-adhesive polymer in order to compare cell responses to individual domains with the effects of a mixture of two different domains of FN. We developed a novel surface modification process that immobilizes the FN binding and cell binding domains of FN, III₁₋₂ and III₉₋₁₀ respectively, to a polymer surface through stable covalent bonds. We also compared our surface modification approach involving III₁₋₂ and III₉₋₁₀ that had been bound to the polyurethane substrate from a 1:1 solution with that of the duplex, III₁₋₂III₉₋₁₀, that was also covalently bonded to the substrate. We found significantly higher cell spreading on III₉₋₁₀ covalently functionalized surfaces than on those where III₉₋₁₀ had been non-specifically adsorbed. Surfaces functionalized individually with III₁₋₂ or III₉₋₁₀ elicit distinct biological responses: III₉₋₁₀ supports cell adhesion and spreading whereas III₁₋₂ does not; interestingly, surfaces functionalized with a 1:1 mixture of III₁₋₂ and III₉₋₁₀ had significantly higher cell adhesion and FN matrix assembly than those functionalized only with III₉₋₁₀, suggesting a synergistic effect of III₁₋₂ to enhance the activity of III₉₋₁₀. Significantly, the 1:1 mixture of bound III₁₋₂ and III₉₋₁₀ was as effective for cell adhesion and spreading and matrix assembly as was the surface bound duplex. These results provide new insights into surface modification of synthetic materials with different functional domains of FN.

Dennes and colleagues showed how acidic surfaces can be activated by zirconium tetra(*tert*-butoxide) for binding of RGD peptides using a maleimide cross linker^{13, 15}. Our study advances the studies by Dennes and co-workers by demonstrating a facile technique for conjugating larger protein domains to zirconium activated polyurethane surfaces using a

nitrophenyl carbonate cross linker. Polyurethane surfaces, functionalized through our approach, had higher surface protein loading than surfaces where proteins were non-specifically adsorbed and these surfaces promoted a more robust biological response with respect to cell spreading. This difference in surface loading and biological activity between conjugated and coated surfaces can be attributed to several factors. Firstly, conjugation is through amino groups of surface-exposed lysine residues, which should have a relatively small effect on overall protein conformation. Secondly, proteins conjugated onto surfaces are more stable than those coated on surfaces. Protein adsorption, can cause protein denaturation on contact with a surface, and adsorbed proteins can be displaced with other proteins in the culture medium or secreted by the cells by competitive adsorption¹². Finally, our study uses proteins in their native form without any prior chemical modification in the final conjugation step. This stands in contrast to surface attachment strategies where polypeptides of FN domains are first modified by converting carboxyl groups to amine-reactive Sulfo-NHS esters²² or where they are tethered to homobifunctional PEG derivatives⁶. The conjugation of terminal amino groups of proteins, which are abundant in many proteins, to surface acid groups makes the approach developed amenable to different polymeric materials and to different protein domains.

The synergistic influence of III₁₋₂ on III₉₋₁₀-cell mediated adhesion was unexpected since isolated III₁₋₂ did not support cell adhesion. A mixture of GST and III₉₋₁₀ had a similar effect as the mixture of III₁₋₂ and III₉₋₁₀ on cell adhesion. One possible explanation is the effect of hydrophobicity or hydrophilicity on cell adhesion. Surfaces immobilized with III₉₋₁₀ alone have a background to the ligand which is the hydrophobic carbonate surface whereas those immobilized with mixtures of GST or III₁₋₂ and III₉₋₁₀, present the integrin binding domain against a background of a hydrophilic protein surface. Studies have shown that the nature of the background of FN immobilized on surfaces influences the affinity between integrins and the immobilized protein, and subsequently cell adhesion²³. In the studies conducted by Keselwosky et al., the more hydrophilic surfaces were reported to have higher cell adhesion than the hydrophobic surfaces. In the III₉₋₁₀ alone case, the background surface carbonate is highly hydrophobic whereas a GST or III₁₋₂ background for III₉₋₁₀ in a mixture is hydrophilic. This may account for the significantly higher cell adhesion on surfaces immobilized with both GST and III₉₋₁₀ or III₁₋₂ and III₉₋₁₀ compared to those with III₉₋₁₀ alone.

Fibroblasts adhere to FN using $\alpha_5\beta_1$ and other RGD-dependent integrins to bind to the III₉₋₁₀ domain and III₁₋₂ contains two FN binding sites². Both fluorescence and immunoblotting studies show higher extracellular matrix FN on surfaces conjugated with both III₁₋₂ and III₉₋₁₀ as opposed to those conjugated with III₉₋₁₀ alone or both GST and III₉₋₁₀ and that this difference decreases with time. It is possible that FN synthesized by fibroblasts as they adhere is able to bind to III₁₋₂, thus providing nucleation points for FN matrix assembly by binding soluble FN secreted by adherent cells. This could then also explain the observation that at early time points, there were more nascent FN fibrils on a surface with a mixture of both III₁₋₂ and III₉₋₁₀ than on a surface with III₉₋₁₀ alone.

Our study demonstrates that FN-binding and cell-binding domains of FN can be covalently and individually attached to a synthetic polymer surface and can be used to influence both

cell adhesion and FN matrix assembly on surfaces. This combinatorial approach differs from other combinatorial approaches, such as those using counter gradients of RGD²⁴ in several aspects. It uses the functional domain, III₉₋₁₀, which has higher affinity and selectivity than RGD⁶⁻⁸. The FN functional domains influence cell adhesion and the assembly of FN in the extracellular matrix and not just adhesion alone. Finally, our study shows strong evidence that mixtures of individually bound functional groups are just as robust in eliciting biological responses as a recombinant polypeptide of multiple functional groups. Our synthetic method enables such systematic variation to address the challenge of multifunctionality and to enhance cell functions on synthetic scaffolds.

Supplementary Material

Refer to Web version on PubMed Central for supplementary material.

Acknowledgments

This study was supported by funding from National Institutes of Health to JES (CA044627 and GM059383). This project was initiated while NWK was supported by the New Jersey Center for Biomaterials through NIBIB Training Program Grant T32EB005583 from the National Institutes of Health. The content is solely the responsibility of the authors and does not necessarily represent the official views of the National Institute Of Biomedical Imaging and Bioengineering or the National Institutes of Health. NWK is grateful to Casey Jones and Kung-Ching Liao for help with surface chemistry and to Ji Young Shim for technical help.

REFERENCES

1. Hynes, RO. Fibronectins. New York: Springer-Verlag; 1990.
2. Mao Y, Schwarzbauer JE. Fibronectin fibrillogenesis, a cell-mediated matrix assembly process. *Matrix Biol.* 2005; 24:389–399. [PubMed: 16061370]
3. Hersel U, Dahmen C, Kessler H. RGD modified polymers: biomaterials for stimulated cell adhesion and beyond. *Biomaterials.* 2003; 24(24):4385–4415. [PubMed: 12922151]
4. Hubbell JA. Biomaterials in tissue engineering. *Biotechnology.* 1995; 13(6):565–576. [PubMed: 9634795]
5. Krishna OD, Kiick KL. Protein- and peptide-modified synthetic polymeric biomaterials. *Biopolymers.* 2010; 94(1):32–48. [PubMed: 20091878]
6. Ghosh K, Ren XD, Shu XZ, Prestwich GD, Clark RA. Fibronectin functional domains coupled to hyaluronan stimulate adult human dermal fibroblast responses critical for wound healing. *Tissue Eng.* 2006; 12:601–613. [PubMed: 16579693]
7. Martino MM, Mochizuki M, Rothenfluh DA, Rempel SA, Hubbell JA, Barker TH. Controlling integrin specificity and stem cell differentiation in 2D and 3D environments through regulation of fibronectin domain stability. *Biomaterials.* 2009; 30(6):1089–1097. [PubMed: 19027948]
8. Petrie TA, Capadona JR, Reyes CD, Garcia AJ. Integrin specificity and enhanced cellular activities associated with surfaces presenting a recombinant fibronectin fragment compared to RGD supports. *Biomaterials.* 2006; 27(31):5459–5470. [PubMed: 16846640]
9. Roy DC, Wilke-Mounts SJ, Hocking DC. Chimeric fibronectin matrix mimetic as a functional growth- and migration-promoting adhesive substrate. *Biomaterials.* 2011; 32:2077–2087. [PubMed: 21185596]
10. Xu J, Bae E, Zhang Q, Annis DS, Erickson HP, Mosher DF. Display of cell surface sites for fibronectin assembly is modulated by cell adherence to (1)F3 and C-terminal modules of fibronectin. *PLoS One.* 2009; 4(1):e4113. [PubMed: 19119318]
11. Singh P, Carraher C, Schwarzbauer JE. Assembly of Fibronectin Extracellular Matrix. *Annu. Rev. Cell Dev. Bi., Vol 26.* 2010; 26:397–419.

12. Mrksich M, Whitesides GM. Using self-assembled monolayers to understand the interactions of man-made surfaces with proteins and cells. *Annu. Rev. Biophys. Biomol. Struct.* 1996; 25:55–78. [PubMed: 8800464]
13. Dennes TJ, Schwartz J. Controlling cell adhesion on polyurethanes. *Soft Matter.* 2008; 4(1):86–89.
14. Jones CM, Donnelly PE, Schwartz J. A nanoscale interface improves attachment of cast polymers to glass. *ACS Appl. Mater. Interfaces.* 2(8):2185–2188. [PubMed: 20690771]
15. Dennes TJ, Hunt GC, Schwarzbauer JE, Schwartz J. High-yield activation of scaffold polymer surfaces to attach cell adhesion molecules. *J. Am. Chem. Soc.* 2007; 129(1):93–97. [PubMed: 17199287]
16. Midwood KS, Carolus MD, Danahy MP, Schwarzbauer JE, Schwartz J. Easy and efficient bonding of biomolecules to an oxide surface of silicon. *Langmuir.* 2004; 20(13):5501–5505. [PubMed: 15986692]
17. Silverman BM, Wiegand KA, Schwartz J. Comparative properties of siloxane vs phosphonate monolayers on a key titanium alloy. *Langmuir.* 2005; 21(1):225–228. [PubMed: 15620307]
18. Leahy DJ, Aukhil I, Erickson HP. 2.0 A crystal structure of a four-domain segment of human fibronectin encompassing the RGD loop and synergy region. *Cell.* 1996; 84:155–164. [PubMed: 8548820]
19. Vakonakis I, Staunton D, Rooney LM, Campbell ID. Interdomain association in fibronectin: insight into cryptic sites and fibrillogenesis. *EMBO J.* 2007; 26:2575–2583. [PubMed: 17464288]
20. Hayman EG, Ruoslahti E. Distribution of fetal bovine serum fibronectin and endogenous rat cell fibronectin in extracellular matrix. *J. Cell Biol.* 1979; 83(1):255–259. [PubMed: 389940]
21. McKeown-Longo PJ, Mosher DF. Binding of plasma fibronectin to cell layers of human skin fibroblasts. *J. Cell Biol.* 1983; 97(2):466–472. [PubMed: 6309861]
22. Doran MR, Frith JE, Prowse AB, Fitzpatrick J, Wolvetang EJ, Munro TP, Gray PP, Cooper-White JJ. Defined high protein content surfaces for stem cell culture. *Biomaterials.* 31(19):5137–5142. [PubMed: 20378164]
23. Keselowsky BG, Collard DM, Garcia AJ. Surface chemistry modulates fibronectin conformation and directs integrin binding and specificity to control cell adhesion. *J. Biomed. Mater. Res. A.* 2003; 66(2):247–259. [PubMed: 12888994]
24. Petty RT, Li HW, Maduram JH, Ismagilov R, Mrksich M. Attachment of cells to islands presenting gradients of adhesion ligands. *J. Am. Chem. Soc.* 2007; 129(29):8966–8967. [PubMed: 17602634]

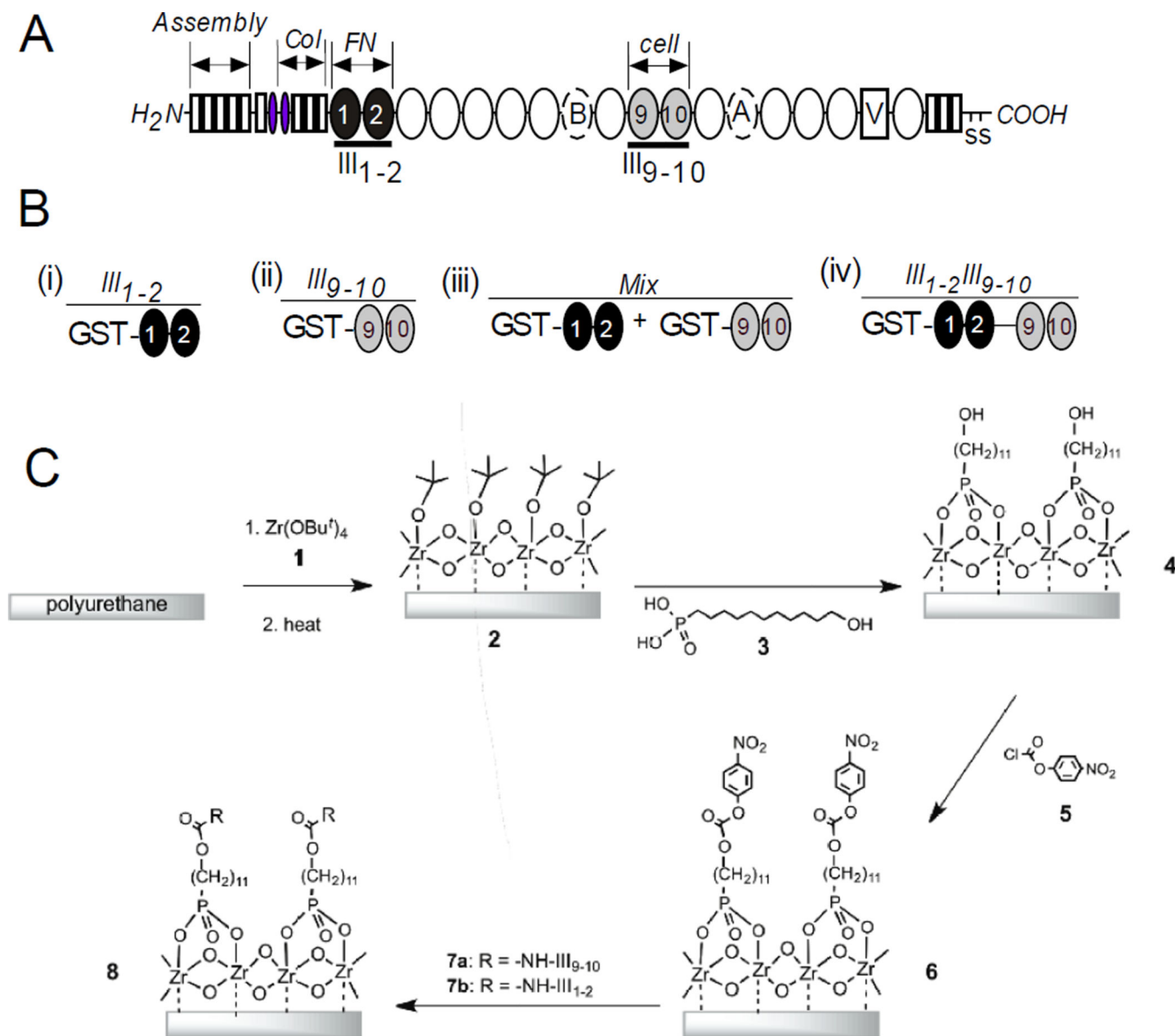


Figure 1.

Functionalization of polyurethane with FN domains. **(A)** Domain structure of FN showing the position of the FN binding domain, III₁₋₂, and the cell-binding domain, III₉₋₁₀ with respect to the amino-terminal assembly domain, the collagen binding domain (Col), the dimerization domain at the carboxyl-terminal (SS), the alternatively spliced A and B domains and the V region. **(B)** Surface chemistry was varied by conjugating GST fusions of the FN- and cell-binding domains of FN, III₁₋₂ and III₉₋₁₀, as individual proteins (i and ii), a mixture of the two domains (iii) or as a fusion of the two domains (iv). **(C)** The carbamate groups of polyurethane were used to coordinate the Zr in a cross-linked alkoxy-oxide (**2**) that was synthesized by vapor deposition of zirconium tetra(*tert*-butoxide) (**1**) followed by heating. This alkoxy-oxide was then used to attach phosphonic acid **3** to polyurethane as surface complex **4**, which was treated with *p*-nitrophenyl chloroformate **5** to give surface

carbonate **6**. The carbonate was then used to attach peptides (**7**) to the surface via a free amino group to yield the bioactive surface **8**.

Author Manuscript

Author Manuscript

Author Manuscript

Author Manuscript

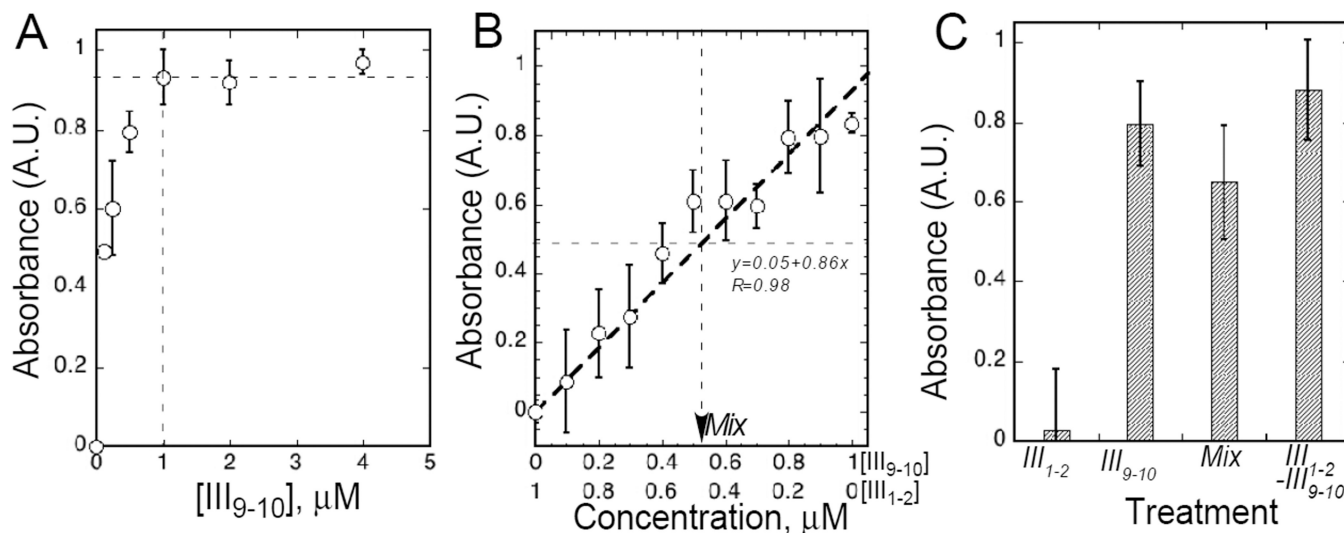


Figure 2.

Characterization of surfaces terminated with III₁₋₂ and III₉₋₁₀ through ELISA. Antibodies specific for III₉₋₁₀ were used to detect these domains on surfaces. (A) Surfaces were incubated with increasing concentrations of III₉₋₁₀ and amount bound was detected by ELISA with HFN7.1 monoclonal antibodies. (B) III₁₋₂ and III₉₋₁₀ were varied in mixtures where total protein concentration was held constant at 1 μM. Bound III₉₋₁₀ was detected by ELISA. Half the maximum III₉₋₁₀ ELISA absorbance is marked and corresponds to 0.5 μM III₁₋₂ and 0.5 μM III₉₋₁₀ (*Mix*). The constants for a linear regression analysis are shown. (C) Analysis of surfaces treated with 0.5 μM III₁₋₂, 0.5 μM III₉₋₁₀, 0.5 μM III₁₋₂ + 0.5 μM III₉₋₁₀ (*Mix*) and 0.5 μM III₁₋₂III₉₋₁₀. Studies were conducted in duplicate, repeated at least three times and normalized to the maximum absorbance in each experiment. The error bars represent a 95% confidence interval of the mean.

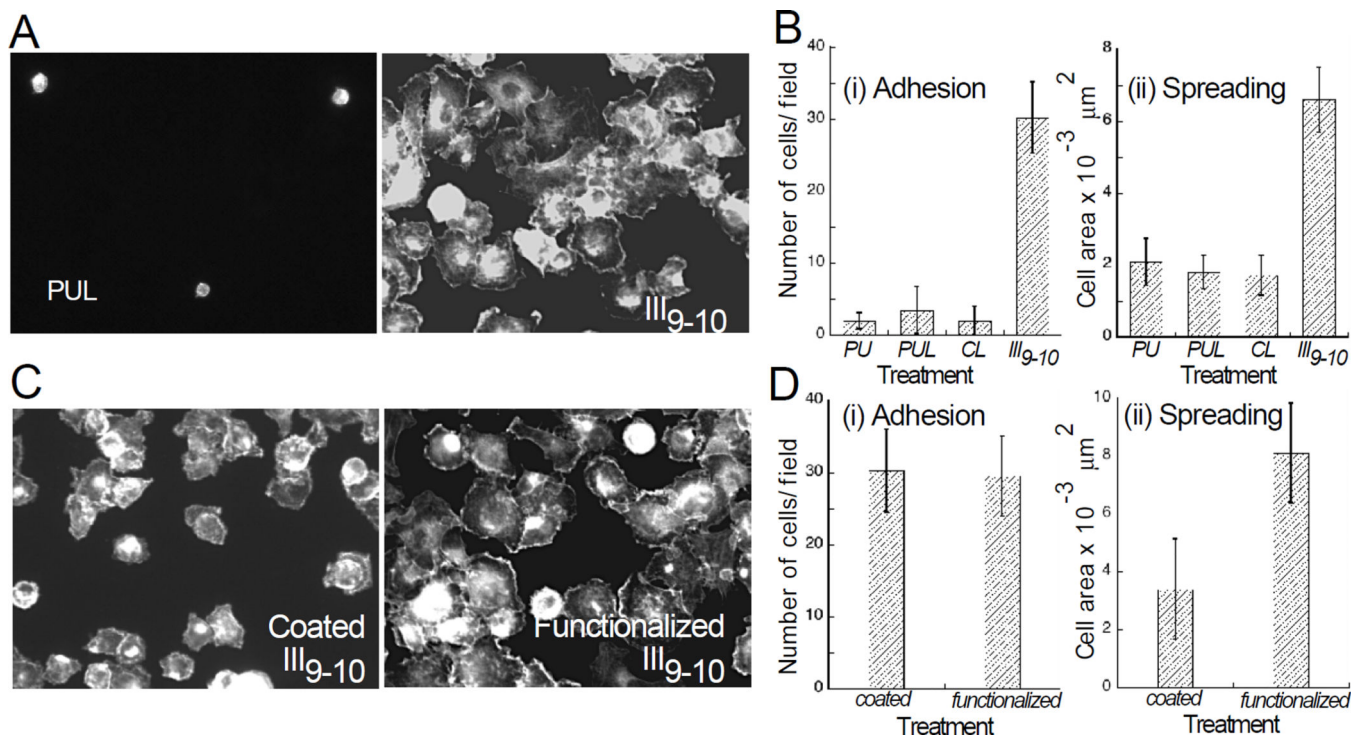


Figure 3. Characterization of functionalized surfaces through cell adhesion and spreading. (A, C) Cells were fixed and stained with fluorescent phalloidin one hour after plating in serum-free medium. (B, D) Quantitative image analysis was used to measure cell adhesion and spreading on surfaces treated as outlined in Figure 1C [PU = polyurethane; PUL = surface 4; CL = nitrophenyl carbonate terminated surface 6; III₉₋₁₀ = surface 8 terminated with III₉₋₁₀].

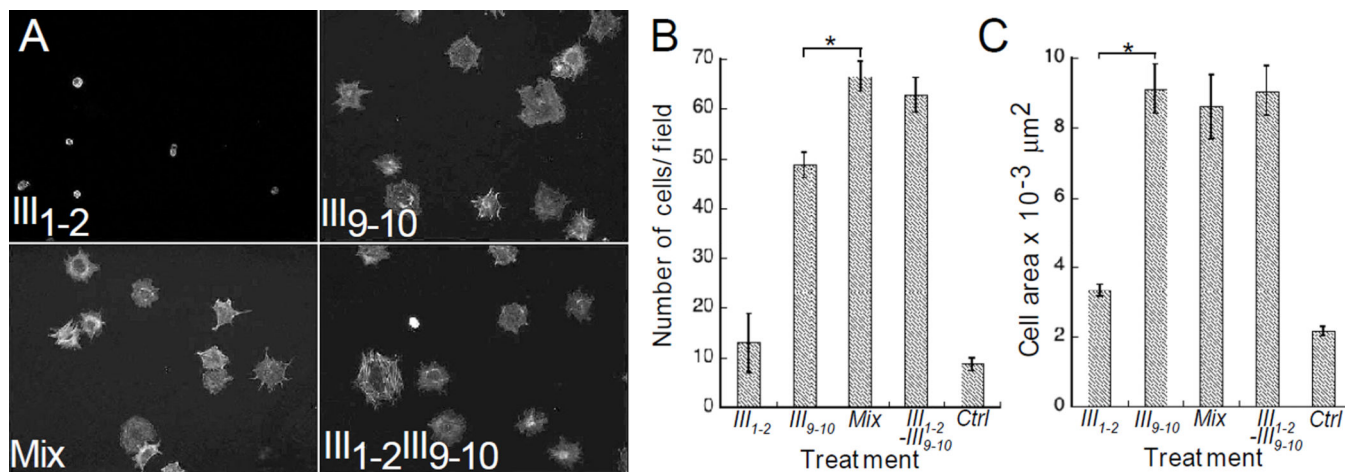


Figure 4.

Cell adhesion and spreading on III₁₋₂ and III₉₋₁₀ functionalized surfaces. (A) Fluorescence images of NIH-3T3 mouse fibroblasts cultured for one hour in serum-free medium, fixed, permeabilized and labeled with fluorescein-phalloidin on III₁₋₂, III₉₋₁₀, III₁₋₂ + III₉₋₁₀ (*Mix*) and III₁₋₂III₉₋₁₀ terminated surfaces. Average cell adhesion (B) and spreading (C) on functionalized surfaces. The control surface (ctrl) in B and C is surface **6** in Figure 1C. The error bars represent the standard errors of the mean of 16 fields in B and 20 to 40 cells in C from two different experiments. ‘*’ marks significantly different means at a 95% confidence interval.

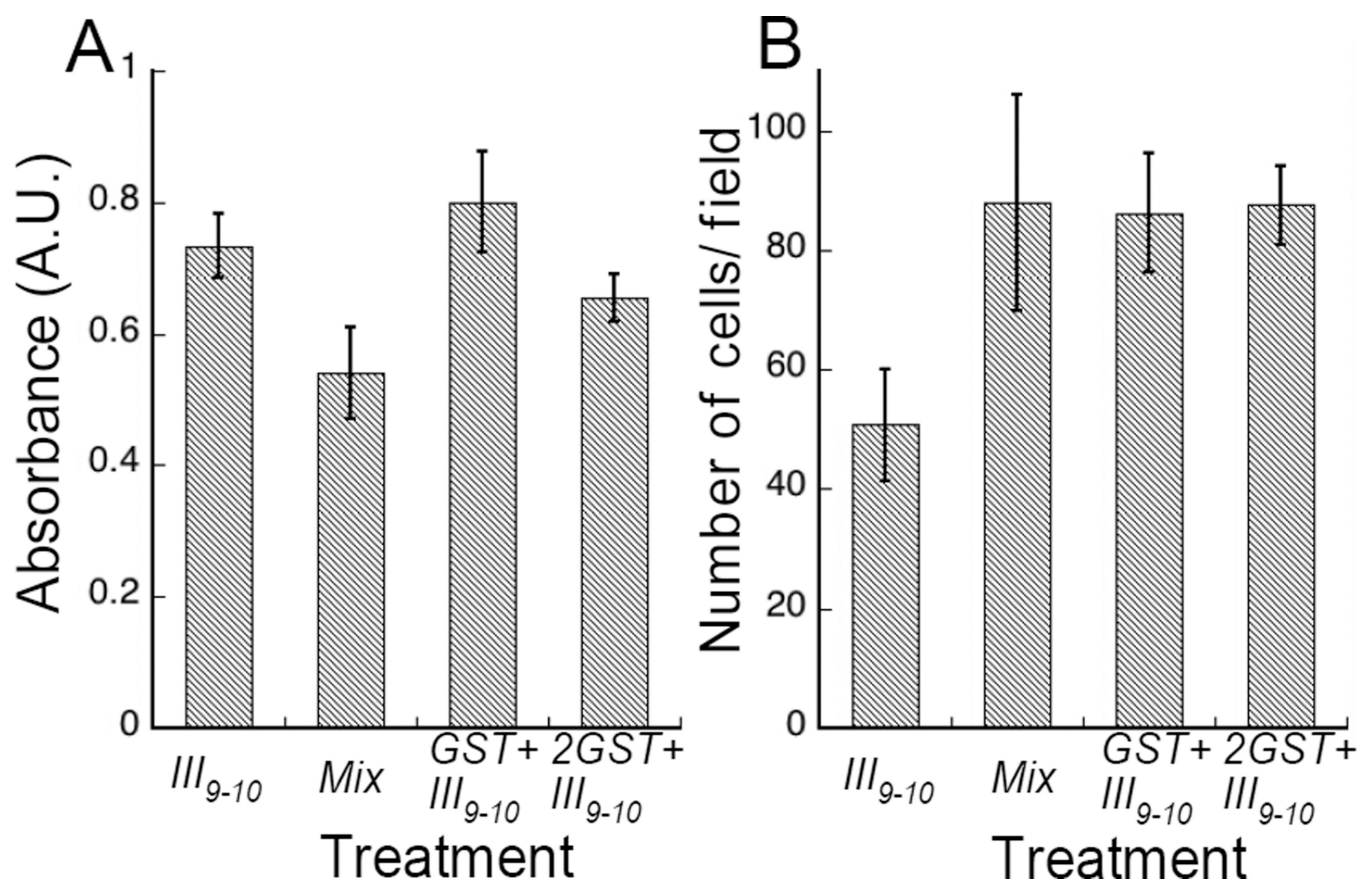


Figure 5.

An analysis of III₁₋₂ potentiation of III₉₋₁₀ activity. Surfaces were conjugated with III₉₋₁₀, mixtures of III₁₋₂ and III₉₋₁₀ (Mix), mixtures of GST and III₉₋₁₀ (GST+III₉₋₁₀ and 2GST+III₉₋₁₀). In “GST+III₉₋₁₀” equal molar concentrations of 0.5 μM GST and 0.5 μM III₉₋₁₀ were present and in “2GST+III₉₋₁₀”, the amount of GST in solution with 0.5 μM III₉₋₁₀ was 1 μM. (A) III₉₋₁₀ ELISA surface detection with HFN7.1 monoclonal antibodies. (B) Average cell adhesion on functionalized surfaces. The error bars in A represent the range of two replicates of two experiments and those in B represent the standard errors of the mean of six fields of studies from two experiments.

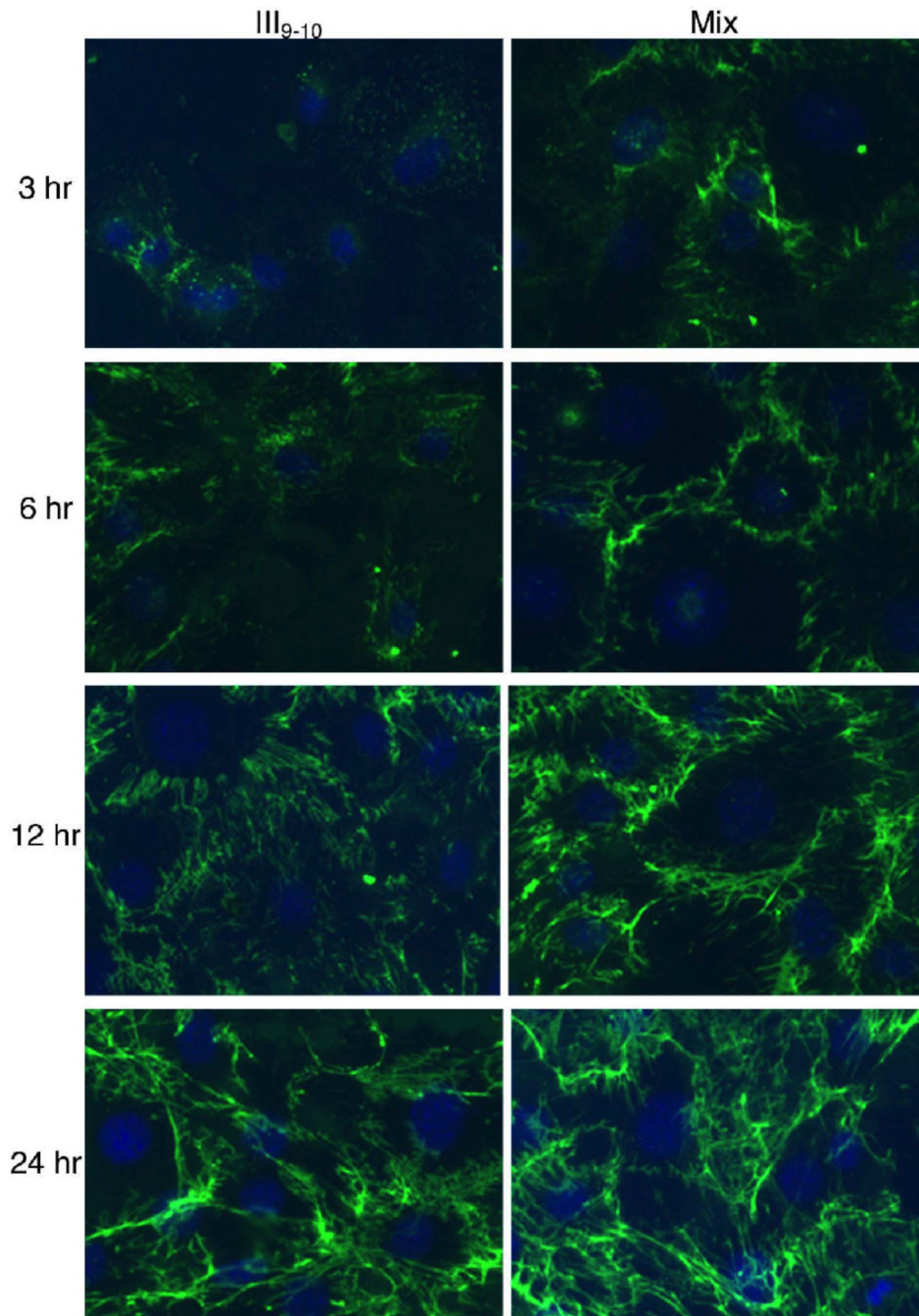


Figure 6. FN fibril formation on functionalized surfaces. NIH3T3 fibroblasts were plated on III₉₋₁₀ or *Mix* surfaces and allowed to assemble FN fibrils for the indicated times. Surfaces were blocked with BSA prior to cell plating. Cells were stained with anti-FN antibodies and Hoechst which binds DNA (blue). The scale bar is 20 μm . All images were collected using the same exposure conditions; hence fluorescence intensity is an indicator of FN content.